Transactions of the **13th International Conference on Structural Mechanics in Reactor Technology** (SMiRT 13), Escola de Engenharia - Universidade Federal do Rio Grande do Sul, Porto Alegre, Brazil, August 13-18, 1995

An inelastic model for thin shell analysis

Brank, B.[1], **Damjanic, F.B.**[1], **Peric, D.**[2]
1) University of Ljubljana, Institute of Structural and Eartquake, Ljubljana, Slovenia
2) University College of Swansea, Dep. of Civil Engineering, Swansea, England

ABSTRACT: A nonlinear finite element formulation for thin elastic shells (Brank et al. 1993) is extended to include plasticity. Constrained three dimensional elastoplastic constitutive equations are used for the purpose. Stress resultants are obtained with through-thickness numerical integration. A return mapping algorithm is adopted for the integration of constitutive equations. Systematic linearization of the algorithm, leading to the consistent elastoplastic tangent modulus is performed. A numerical example is presented to illustrate the formulation.

1 INTRODUCTION

In shell theory two different approaches can be adopted for the formulation of inelastic constitutive equations. The first one, also applied in the present work, uses three dimensional stress-strain laws, which are modified by enforcing the constraints present in shell theory. In particular, when the classical thin shell models are considered (e.g. Büchter and Ramm 1992), the component of Cauchy stress tensor in the thickness direction is assumed to vanish. If the theory is restricted to small strains, this assumption may be applied to the component of the second Piola-Kirchhoff stress tensor, i.e. $S^{33} = 0$. As a consequence, the condensation of the three dimensional material law is required. This is trivial in the case of linear elasticity, but it may be very demanding for certain nonlinear material formulations. In elastoplasticity the condensation may be performed explicitly, as presented by Ramm and Matzenmiller (1988), or implicitly (in the computational process) as suggested by de Borst (1991). The stress constraints also place nontrivial constraints on the standard return mapping algorithms as shown by Simo and Taylor (1986). Using the first approach the stress resultants are obtained by integration of stresses through the thickness. On the other hand, the second approach formulates constitutive models directly in stress resultants and circumvents the need for stress integration. Such models were recently presented by Simo and Kennedy (1992) and Crisfield and Peng (1992). In that case the diffusion of the plasticity through the thickness cannot be traced. Moreover, it is not a simple task to perform analytical reduction of complex three dimensional constitutive equations to stress resultant form. An important computational aspect of any elastoplastic model is a systematic linearization of the adopted integration algorithm in order to get consistent tangent modulus.

2 KINEMATIC RELATIONS

Adopting a classical point of view, any possible configuration of the shell is determined in terms of two objects (see e.g. Büchter and Ramm 1992 or Simo and Kennedy 1992): a surface parametrized by a map $\varphi : A \rightarrow R^3$, so that

$$M = \left\{ \mathbf{r} \in R^3 : \mathbf{r} = \varphi \left(\xi^1, \xi^2\right) \text{ for } \left(\xi^1, \xi^2\right) \in A \right\} \quad (1)$$

and one vector field on M, denoted by $\overline{\mathbf{d}}$. Basic kinematic assumption is, that any placement of the shell, $S \subset R^3$, is given as

$$S = \left\{ \mathbf{x} \in R^3 : \mathbf{x} = \mathbf{r} + \xi \mathbf{d}, \quad \xi \in [-H/2, H/2] \right\} \quad (2)$$

where $\|\mathbf{d}\| = 1$, H is shell thickness at the initial (stress-free) configuration and $\mathbf{d} = \overline{\mathbf{d}} \circ \varphi$. Using (2), the metric tensors at the deformed and initial configuration, as well as symmetric Green-Lagrange strain tensor, $\mathbf{E}$, may be derived. Approximating terms describing the shell geometry, the strain tensor components may be given as

$$E_{\alpha\beta} = \varepsilon_{\alpha\beta} + \xi \kappa_{\alpha\beta}, \quad E_{\alpha 3} = E_{3\alpha} = 1/2\gamma_\alpha, \quad E_{33} = 0 \quad (3)$$

$$\varepsilon_{\alpha\beta} = 1/2 \left(\mathbf{r}_{,\alpha} \cdot \mathbf{r}_{,\beta} - \mathbf{r}^0_{,\alpha} \cdot \mathbf{r}^0_{,\beta} \right), \quad \gamma_\alpha = \left(\mathbf{r}_{,\alpha} \cdot \mathbf{d} - \mathbf{r}^0_{,\alpha} \cdot \mathbf{d}^0 \right) \quad (4)$$

$$\kappa_{\alpha\beta} = 1/2 \left(\mathbf{d}_{,\alpha} \cdot \mathbf{r}_{,\beta} + \mathbf{d}_{,\beta} \cdot \mathbf{r}_{,\alpha} - \mathbf{d}^0_{,\alpha} \cdot \mathbf{r}^0_{,\beta} - \mathbf{d}^0_{,\beta} \cdot \mathbf{r}^0_{,\alpha} \right) \quad (5)$$

Quantities with superscript ^{0} are related to the initial configuration and $\mathbf{r} = \mathbf{r}^0 + \mathbf{u}$, where $\mathbf{u}$ defines a vector (displacement) field on M^0. The shell director, $\overline{\mathbf{d}}$, at a particular point $\mathbf{r} \in M$, can be completely described by two Euler angles (Fig. 1a). For details we refer to Büchter and Ramm (1992) and Brank et al. (1993).

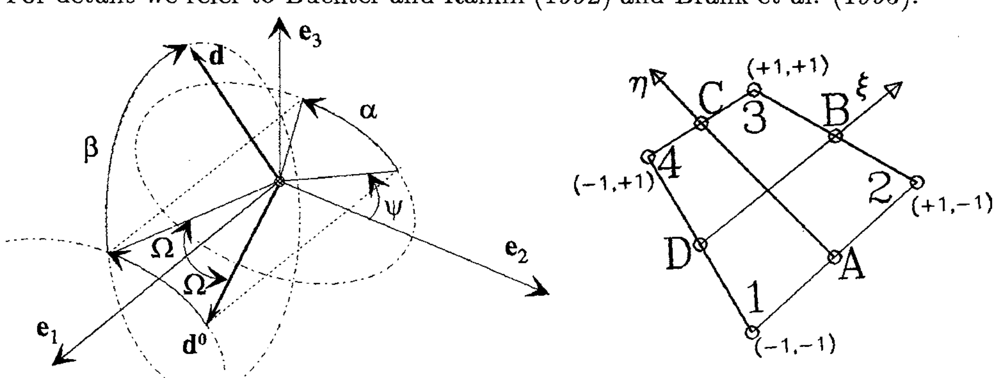

Fig 1. a) Shell director at material and spatial configuration. b) 4-node element.

3 CONSTITUTIVE EQUATIONS

The classical three dimensional elastoplastic constitutive equations may be formulated as (e.g. Lemaitre and Chaboche 1990)

$$\mathbf{E} = \mathbf{E}^e + \mathbf{E}^p \quad (6)$$

$$W\left(\mathbf{E}^e, \mathbf{R}\right) = W^e\left(\mathbf{E}^e\right) + W^p\left(\mathbf{R}\right) \quad (7)$$

$$\mathbf{S} = \partial_{\mathbf{E}^e} W^e, \qquad \mathbf{K} = \partial_{\mathbf{R}} W^p \tag{8}$$

$$\Phi = \Phi(\mathbf{S}, \mathbf{K}) \tag{9}$$

$$\dot{\mathbf{E}}^p = \gamma \partial_{\mathbf{S}} \Phi(\mathbf{S}, \mathbf{K}), \qquad -\dot{\mathbf{R}} = \gamma \partial_{\mathbf{K}} \Phi(\mathbf{S}, \mathbf{K}) \tag{10}$$

$$\gamma \geq 0, \quad \Phi \leq 0, \quad \gamma \Phi = 0 \quad \text{and} \quad \gamma \dot{\Phi} = 0 \quad \text{if} \quad \Phi = 0 \tag{11}$$

Eq. (6) assumes that the deformation tensor additively decomposes into an elastic and a plastic part. It is further assumed that the stress response is characterized by a specific free energy function (7), given as a sum of two functions. **R** represents internal (strain-like) variables, associated with a hardening response of the material and **K** are thermodynamical forces conjugated to **R**. Stress constitutive equations (8) follow from the second law of thermodynamics. **S** is the second Piola-Kirchhoff stress tensor. The plastic response is characterized by a yield function (9), formulated in stress space. Eqs. (10) assume an associative flow rule and a hardening law. In eqs. (10) γ denotes the plastic consistency parameter which is assumed to obey the Kuhn-Tucker complementary conditions (11) and consistency requirement $(11)_4$.

When explicit enforcement of the zero-through-thickness-stress-component constraint, $S^{33} = 0$, is performed, eqs. (6-10) need to be modified. For that purpose it is convinient to introduce matrix notation as shown by Simo and Taylor (1986) and Ramm and Matzenmiller (1988) for J_2 plasticity.

4 BOUNDARY VALUE PROBLEM

The material version of the equilibrium of the shell may be established by the principle of virtual work

$$G(\mathbf{S}, \mathbf{x}, \delta\mathbf{x}) = \int_{M^0} \left(n^{\alpha\beta} \delta\varepsilon_{\alpha\beta} + m^{\alpha\beta} \delta\kappa_{\alpha\beta} + q^{\alpha} \delta\gamma_{\alpha} \right) dM^0 - G_{ext}(\delta\mathbf{x}) = 0 \tag{12}$$

where the stress resultants are defined as ($\mu dz = dS^0 / dM^0$)

$$n^{\alpha\beta} = \int_{\frac{-H}{2}}^{\frac{H}{2}} S^{\alpha\beta} \mu dz, \quad m^{\alpha\beta} = \int_{\frac{-H}{2}}^{\frac{H}{2}} S^{\alpha\beta} z \mu dz, \quad q^{\alpha} = \int_{\frac{-H}{2}}^{\frac{H}{2}} S^{\alpha 3} \mu dz \tag{13}$$

Further assume that $\mathbf{E}^p$ and $\mathbf{R}$ are known at a certain time t_n. The deformation at a subsequent time t_{n+1} will determine the value of **S** at t_{n+1} through the integration algorithm (Section 5). This defines the (algorithmic) incremental constitutive relation $\mathbf{S}_{n+1} = \mathbf{S}(\mathbf{E}^p_n, \mathbf{R}_n, \mathbf{x}_{n+1})$. Once $\mathbf{S}_{n+1}$ is known, the stress resultants at t_{n+1} can be evaluated with (13). Accordingly, the incremental boundary value problem can be stated as: Given $\mathbf{E}^p_n$ and $\mathbf{R}_n$ at t_n, and loading conditions at t_{n+1}, find a configuration $\mathbf{x}_{n+1}$, such that (12) holds at t_{n+1}. To solve (12) at t_{n+1} with Newton-Raphson iterative procedure, its linearization about a certain configuration $\mathbf{x}^{(i)}_{n+1}$, has to be performed

$$\left[D_M G\left(\mathbf{x}^{(i)}_{n+1}, \delta\mathbf{x}\right) + D_G G\left(\mathbf{x}^{(i)}_{n+1}, \delta\mathbf{x}\right) \right] \cdot \Delta\mathbf{x}^{(i)}_{n+1} = -G\left(\mathbf{x}^{(i)}_{n+1}, \delta\mathbf{x}\right) \tag{14}$$

The geometric part of the tangent operator, $D_G G$, has the same form as in the purely elastic case, except that the stress resultants are evaluated by elastoplastic constitutive equations. On the other hand, the material part, $D_M G$, takes a different form. For its evaluation the consistent (algorithmic) tangent modulus, $d\mathbf{S}_{n+1}^{(i)}/d\mathbf{E}_{n+1}^{(i)}$, is required. Once specified and integrated across the thickness according to (13), the consistent tangent operator becomes completely defined.

5 NUMERICAL INTEGRATION ALGORITHM

The implementation of the (implicit) backward Euler algorithm for the integration of constitutive eqs. (6-11) may be briefly summarized in the following steps:

1. At the begining of the time step $[t_n, t_{n+1}]$, the following data are known: $\mathbf{E}_n, \mathbf{E}_n^p, \mathbf{R}_n$ and $\mathbf{E}_{n+1}$.

2. Set $\gamma_{n+1} = 0$ and evaluate trial elastic stresses $\mathbf{S}_{n+1}^e = \partial_{\mathbf{E}_{n+1}^e} W_{n+1}^e$, where $\mathbf{E}_{n+1}^e = \mathbf{E}_{n+1} - \mathbf{E}_n^p$.

3. Check whether the time step is elastic, i.e. check if the condition $(11)_2$ is violated: (a) if $\Phi\left(\mathbf{S}_{n+1}^e\right) \leq 0$, set $\mathbf{S}_{n+1} = \mathbf{S}_{n+1}^e$, $\mathbf{E}_{n+1}^p = \mathbf{E}_n^p$, $\mathbf{R}_{n+1} = \mathbf{R}_n$ and exit; (b) if $\Phi\left(\mathbf{S}_{n+1}^e\right) > 0$, go to 4 and perform the return map.

4. Solve a sistem of nonlinear algebraic equations with $\mathbf{E}_{n+1}^e$, $\mathbf{R}_{n+1}$ and γ_{n+1} as the unknowns. If yield function, Φ, and both parts of the specific free energy function, W^e and W^p, are of a quadratic form, a single nonlinear scalar equation, $\Phi_{n+1}(\gamma_{n+1}) = 0$, has to be solved.

5. Update plastic strains $\mathbf{E}_{n+1}^p = \mathbf{E}_{n+1} - \mathbf{E}_{n+1}^e$ and stresses $\mathbf{S}_{n+1} = \partial_{\mathbf{E}_{n+1}^e} W_{n+1}^e$.

The above algorithm can be also used when explicit enforcement of the zero-through-thickness-stress-component constraint is performed. In that case the matrix notation should be employed; see Ramm and Matzenmiller (1988) for J_2 plasticity.

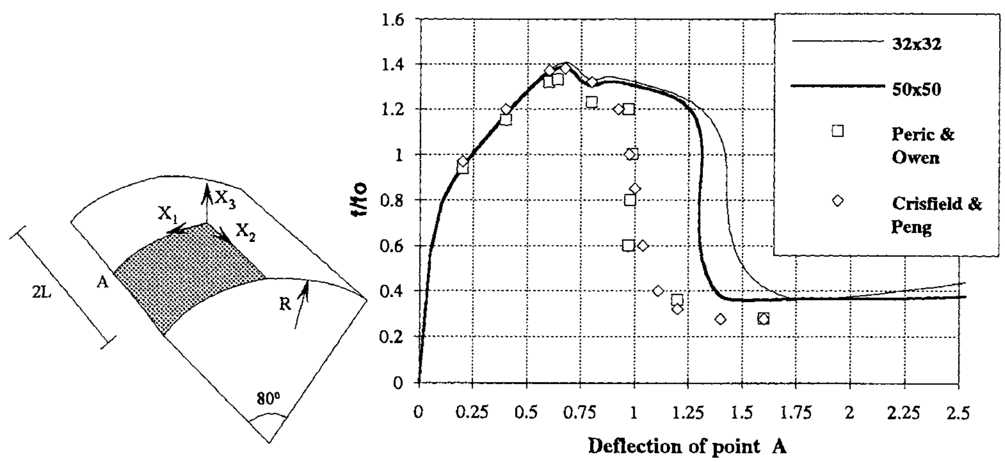

Fig 2. Scordelis-Loo roof: a) geometry, b) load-displacement curves for point A.

6 FINITE ELEMENT DISCRETIZATION

In the approximation of the incremental problem the finite element method is used in a standard manner. A four node isoparametric shell finite element is developed (Fig. 1b). The geometry, kinematic variables, incremental and varied quantities are interpolated by bilinear functions. In addition, to avoid shear locking, the transverse shear strain field is given by constant-linear interpolation (see Brank et al. 1993 and Refs. therein for details). In the present formulation the chosen interpolation and linearization commute.

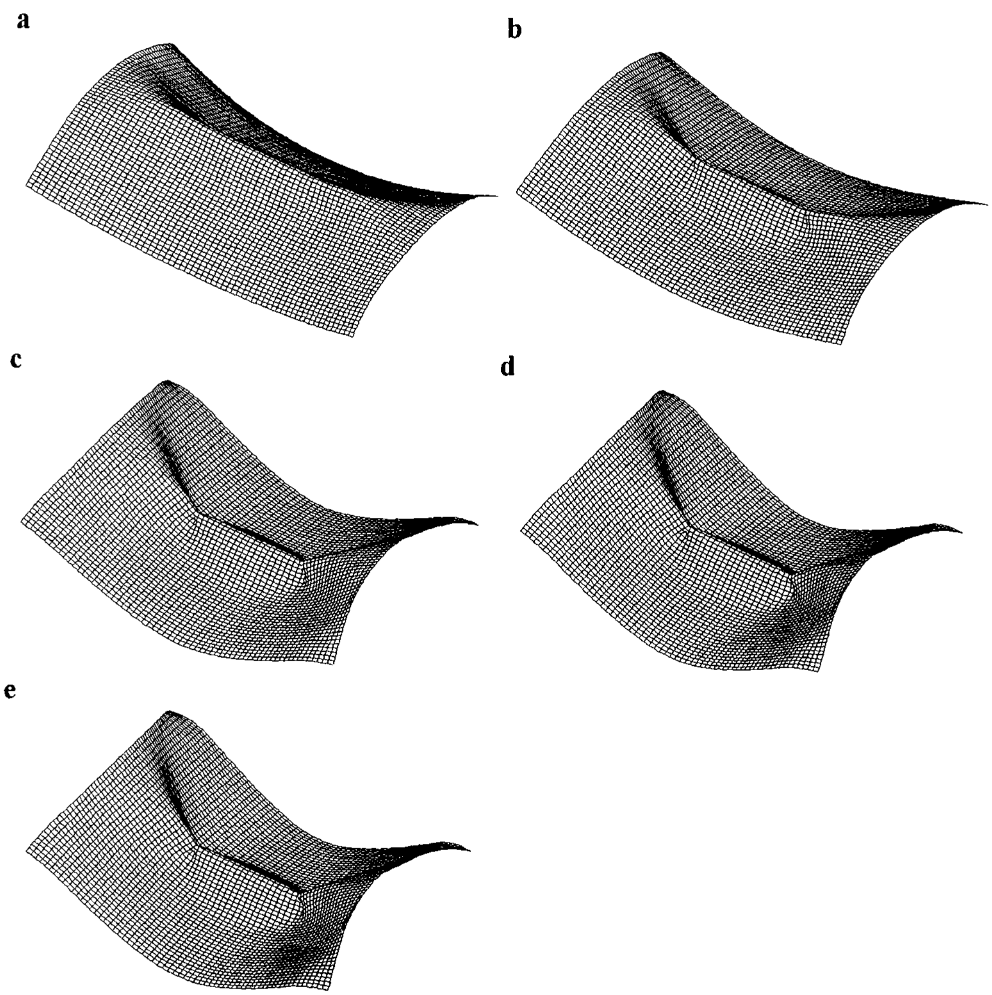

Fig 3. Deformed finite element meshes (32×32). Displacement U_3 at point A is: a) -1.3850 m, b) -1.5736 m, c) -2.6073 m, d) -2.8860 m and e) -3.2234 m.

7 NUMERICAL EXAMPLE

Failure analysis of Scordellis-Loo roof is considered. The geometry and material characteristics of the problem are defined as (Fig. 2a): One half of the length equals to radius, $L = R = 7.6$ m, thickness is $t = 0.076$ m, elastic modulus is $E = 2.1 \times 10^4$ N/mm^2, Poisson's ratio is $\nu = 0.0$, yield stress is $S_y = 4.2$ N/mm^2 and hardening parameter is $H = 0.0$. Von Mises yield function is adopted. The loading, f, acts on the shell as a self weight. Its initial value is $f_0 = 4.0$ kN/m^2. Symmetry conditions allow the analysis of one quarter of the roof. The example has been studied by different authors. The most complete nonlinear analyses have been done by Perić and Owen (1991) and Crisfield and Peng (1992). The authors of both references used the faceted shell formulations based on Morley's thin shell triangular elements. In the present computations two different meshes of 32×32 and 50×50 four node elements were used. Simpson's integration rule with 7 integration points was employed for the numerical integration accross the thickness. Load versus vertical displacement curves for point A are plotted in Fig. 2b. The curves of both meshes are virtually the same and compare well with the results of mentonied references prior the maximum load. This, however, cannot be said for the section of unstable equilibrium configurations. A sharp drop, observed in all diagrams, occures at $U_3 \approx -1.0$ in Perić and Owen (1991) and Crisfield and Peng (1992), while it is noticed at $U_3 \approx -1.3$ in the present analysis. The differences in diagrams may relate to the differences in the finite element formulations. The very localised failure mode of the roof is evident from Fig. 3, where five equilibrium configurations are shown.

8 CONCLUSION

Constrained three dimensional elastoplastic constitutive equations are employed into the earlier developed geometrically nonlinear formulation for thin shells. Systematic linearization of the adopted model has been performed, leading to an efficient numerical algorithm with quadratic rate of asymptotic convergence. The numerical example illustrates the potential use of the model for the analysis of practical problems (e.g. pipes, tanks, containers etc.).

REFERENCES

de Borst,R. 1991. The zero-normal-stress condition in plane-stress and shell elastoplasticity. *Comm. Appl. Numer. Meth.* 7:29-33.

Brank,B., D. Perić & F.B.Damjanić 1993. A nonlinear four node shell element with explicit integration and elementary rotations. In *Proc. Trans. of the 12th Int. Conf. SMIRT, B*:153-158. Amsterdam: Elsevier Science Publ.

Büchter,N. & E.Ramm 1992. Shell theory versus degeneration - a comparison in large rotation finite element analysis. *Int. J. Numer. Meth. Engng.* 34:39-59.

Crisfield,M.A. & X.Peng 1992. Efficient non-linear shell formulations with large rotations and plasticity. In *Proc. 3rd Int. Conf. on Computational Plasticity,* 1979-1996. Swansea: Pineridge Press.

Lemaitre,J. & J.-L. Chaboche 1990. *Mechanics of solid materials.* Cambridge University Press.

Perić,D. & D.R.J.Owen 1991. The Morley thin shell finite element for large deformations problems: simplicity versus sophistication. In *Proc. Int. Conf. on Nonlinear Engineering Computations,*121-142. Swansea: Pineridge Press.

Ramm,E. & A.Matzenmiller 1988. Consistent linearization in elasto-plastic shell analysis. *Eng. Comput.* 5:289-299.

Simo,J.C. & R.L.Taylor 1986. A return mapping algorithm for plane stress elastoplasticity. *Int. J. Numer. Meth. Engng.* 22:649-670.

Simo,J.C. & J.G.Kennedy 1992. On a stress resultant geometrically exact shell model. Part V. Nonlinear plasticity: formulation and integration algorithms. *Comp. Meth. Appl. Mech. Eng.* 96:133-171.